Modeling the Biosphere–Atmosphere System: The Impact of the Subgrid Variability in Rainfall Interception

GUILING WANG AND ELFATIH A. B. ELTAHIR

Ralph M. Parsons Laboratory, Department of Civil and Environmental Engineering, Massachusetts Institute of Technology, Cambridge, Massachusetts

(Manuscript received 25 May 1999, in final form 21 October 1999)

ABSTRACT

Subgrid variability in rainfall distribution has been widely recognized as an important factor to include in the representation of land surface hydrology within climate models. In this paper, using West Africa as a case study, the impact of the subgrid variability in rainfall interception on the modeling of the biosphere–atmosphere system is investigated. According to the authors' results, when neglecting the rainfall spatial variability, even if the impact on the total evapotranspiration is negligible, significant errors may result in the representation of surface hydrological processes and surface energy balance. These findings are consistent with the results of previous studies. However, in this paper, this issue is further explored and it is demonstrated that the extent of the resulting errors is not limited to the land surface processes. They extend to the atmosphere via the low-level cloud feedback to impact solar radiation, boundary layer energy, atmospheric circulation, and the distribution of precipitation. The same errors also propagate into the biosphere through vegetation dynamics and can eventually lead to a significantly different biosphere–atmosphere equilibrium state. This study provides a good example for the need to have physical realism in modeling the subgrid variability and most other details of the complex biosphere–atmosphere–ocean system.

1. Introduction

Representation of surface hydrology has become an important component of climate models for its impact on the energy and water balance at the land surface. In the past few decades, as land surface parameterization schemes developed toward greater physical realism, it has been widely recognized that the spatial variability in precipitation and land surface properties (e.g., vegetation type and soil texture) at the subgrid scale significantly affects the simulation of surface hydrological processes at the grid scale (Entekhabi and Eagleson 1989; Pitman et al. 1990; Lloyd 1990; Seth et al. 1994; Ghan et al. 1997; Giorgi and Avissar 1997). Among these factors, the subgrid variability of precipitation has the first-order effect since it serves as the main forcing for surface hydrological processes (Shuttleworth 1988; Ghan et al. 1997). Even if the vegetation and soil are homogeneous, the spatial variability in precipitation still significantly affects the dynamics of water storage including soil moisture and canopy water. Here we focus on the importance of representing subgrid variability of precipitation in climate models.

Corresponding author address: Dr. G. Wang, Ralph M. Parsons Laboratory, 48-208, Dept. of Civil and Environmental Engineering, Massachusetts Institute of Technology, Cambridge, MA 02139.
E-mail: GuilingWang@alum.mit.edu

The impact of subgrid variability of rainfall is most pronounced in the Tropics, where the vegetation canopy is dense and most of the precipitation takes place as convective rainfall. A typical convective rain cell has a spatial coverage of about 10^2-10^3 km^2 (e.g., Rodriguez-Iturbe and Eagleson 1987; Pitman et al. 1990), while a typical grid cell in a climate model often covers the area of 10^3-10^6 km^2. Without considering the impact of this scale mismatch, many climate models predict drizzle uniformly falling over the entire grid area instead of intense rainfall concentrated in a small portion of the grid cell (Pitman et al. 1990). As a result, more rainfall is intercepted by the vegetation canopy and subsequently reevaporated (Pitman et al. 1990; Lean and Warrilow 1989; Dolman and Gregory 1992; Eltahir and Bras 1993a). To avoid such a crude representation of canopy hydrology, an interception scheme that accounts for the subgrid variability of rainfall is necessary. One commonly used approach in interception schemes is the ''statistical approach'' (e.g., Shuttleworth 1988), which combines the point description of canopy hydrology and the statistical treatment of rainfall subgrid variability. This approach assumes that precipitation covers only a fraction μ of the grid cell, and assumes an idealized function for the precipitation probability distribution within the rain-covered region (Carson 1986; Shuttleworth 1988; Eltahir and Bras 1993a). The grid-averaged interception loss and throughfall are then computed

based on these assumptions. The impact of subgrid variability is therefore implicitly represented by modifying the grid-average values for hydrologic variables of local relevance. Another commonly used approach is the ''mosaic approach'' (e.g., Avissar and Pielke 1989; Koster and Suarez 1992a,b; Seth et al. 1994), which explicitly breaks each grid cell into certain number of smaller cells and is frequently used when the heterogeneity of land surface properties (e.g., vegetation and soil) is also considered.

The impact of rainfall subgrid variability on surface processes has been investigated by many studies (Pitman et al. 1990; Eltahir and Bras 1993a; Seth et al. 1994; Ghan et al. 1997) using sophisticated land surface models such as Biosphere–Atmosphere Transfer Scheme (BATS) (Dickinson et al. 1993). While Eltahir and Bras (1993a) focused on the estimation of canopy interception, other studies paid more attention to the energy and water balance of the overall land surface. According to Pitman et al. (1990), changing the areal distribution of precipitation alters the balance between runoff and evaporation. In their study, modifying the rain-covered area can change the surface climatology from an evaporation-dominated regime into a runoff-dominated regime. Consistently, Seth et al. (1994) showed that considering the rainfall subgrid variability affects the energy partitioning and modifies the Bowen ratio. A study by Ghan et al. (1997) showed that neglecting the subgrid variability in summer precipitation caused a decrease of runoff by 48% and increase of evapotranspiration by 15%. A common conclusion can be drawn from these studies that the subgrid variability of rainfall or the lack of it significantly affects the water partitioning between evapotranspiration and runoff as well as the partitioning of the radiative energy input between the sensible heat and latent heat fluxes at the land surface.

Most of the previous studies on the impact of rainfall subgrid variability used offline land surface models, where the atmospheric forcings were prescribed. It is not obvious how the atmospheric feedback, when included, would modify the sensitivity of surface processes to changes in the representation of rainfall interception (Kim and Entekhabi 1998). Dolman and Gregory (1992) investigated this issue using a 1D version of the the U.K. Meteorological office 11-layer GCM with a simple land surface scheme. They found that the total evapotranspiration in the model is strongly controlled by the radiation input and is rather insensitive to the representation of rainfall interception. In their study, when the rain-covered fraction changes from 0.1 to 0.3, the total amount of evapotranspiration differs by only 1%, which implies that the parameterization of rainfall subgrid variability affects only the partitioning between direct evaporation from the canopy storage and plant transpiration, but not the total evapotranspiration.

In addition to the contradiction between the results of studies using offline models and those using coupled models, previous studies have been limited to the impact of subgrid variability on the surface hydrological processes. Its broader effect has not been evaluated. Even if the total evapotranspiration remains the same, the incorrect partitioning between the evaporation and plant transpiration may still have a significant impact on the terrestrial biosphere–atmosphere system through the cloud feedback as well as vegetation physiological and dynamical processes (Wang and Eltahir 1998). In addition, no previous study has looked at the issue of subgrid variability in the context of a dynamic terrestrial biosphere, which evolves in time under the corresponding atmospheric forcings.

Here, using West Africa as a case study, we investigate the impact of the subgrid variability in rainfall interception on the modeling of the biosphere–atmosphere system using a coupled dynamic model. The model simulates not only the land surface processes, but also the atmospheric and terrestrial biospheric processes. We first document the errors in the simulation of land surface hydrological processes caused by the neglect of the subgrid variability in rainfall interception. We then demonstrate how these errors propagate through the atmospheric and biospheric processes, and how they influence the biosphere–atmosphere equilibrium. Section 2 describes the model used in this study, emphasizing the components that are closely related to the current topic. Section 3 describes the two fundamental experiments performed in this study, one assuming uniform rainfall distribution within each grid cell and one assuming variable rainfall distribution. Results from these two experiments and their interpretations are presented in section 4. Section 5 demonstrates the role of the cloud feedback in propagating the errors caused by the neglect of the subgrid variability in rainfall interception, which illustrates the analyses of section 4. In section 6, we address the error propagation through vegetation dynamics. Section 7 presents the discussion and conclusions.

2. Model description

In this study, we use a zonally symmetric biosphere–atmosphere model (ZonalBAM), which assumes uniform conditions in the zonal direction. It was designed for studying the biosphere–atmosphere interactions over West Africa (Wang and Eltahir 2000a,b), where the high degree of zonal symmetry in climate conditions justifies the use of a zonally symmetric model for climate simulations (Zheng and Eltahir 1997, 1998). The model combines a zonally symmetric atmospheric model and a fully dynamic biospheric model, and has been carefully tested against observations (Wang and Eltahir 2000a). The atmospheric model includes the representation of atmospheric dynamics, a radiation scheme, a moist convection scheme, a boundary layer scheme, and a cloud parameterization scheme. The biospheric model uses the Integrated Biosphere Simulator (IBIS) (Foley

et al. 1996), which integrates a wide range of terrestrial phenomena, including the biophysical, physiological, and ecosystem dynamical processes, into a single, physically consistent simulator. IBIS consists of four component modules: the land surface module, the vegetation phenology module, the carbon balance module, and the vegetation dynamics module. To account for the impact of the rainfall subgrid variability, we have incorporated into IBIS a canopy interception scheme, which is described in section 2c.

Land surface processes are the most relevant to this study. As will be shown later, the cloud feedback and vegetation dynamics are important physical processes in propagating the errors associated with the inaccurate representation of rainfall interception. Therefore, in the following we describe in detail the cloud parameterization scheme of the atmospheric model, the land surface module, and vegetation dynamics module of the biospheric model, as well as the canopy interception scheme.

a. Cloud parameterization scheme

Our model takes a highly simplified approach toward the representation of clouds. Three types of clouds are considered in this model: high-level clouds, medium-level clouds, and low-level clouds. The horizontal expansion of each cloud type, that is, the fractional cloud cover, is predicted by the model. However, other properties of the clouds, including the vertical expansion and the optical depth, are fixed. We assume the vertical expansion to be 640–940 mb for low clouds, 460–640 mb for medium clouds, and 220–460 mb for high clouds, and assume the optical depth to be 12, 6, and 2 for low, medium, and high clouds, respectively (London 1952).

The parameterization of the fractional cloud cover is developed based on Kvamsto (1991), which features a linear relationship between the relative humidity and the fractional cover of the low-level clouds, as described by the following:

$$\mathrm{FC} = \max\left(0.0, \frac{\mathrm{RH} - \mathrm{RH}_0}{1 - \mathrm{RH}_0}\right), \tag{1}$$

where FC is the cloud fractional cover, RH is the relative humidity, and RH_0 is the relative humidity threshold at which clouds start to form. Despite of its simplicity, the performance of the Kvamsto scheme is one of the best among the seven schemes examined by Mocko and Cotton (1995). We adapt the linear scheme shown in Eq. (1) for the low-level clouds and expand its application to the medium- and high-level clouds. For the relative humidity threshold RH_0, we use 0.80, 0.65, and 0.70 for high-, medium-, and low-level clouds, respectively.

b. Land surface module

The land surface module in IBIS (Foley et al. 1996) represents the biophysical and physiological processes taking place at the land surface, and was developed based on the land surface transfer scheme LSX (Pollard and Thompson 1995). Two vegetation canopy layers, the upper canopy and lower canopy, are considered. Trees exist in the upper canopy, while herbaceous plants occupy the lower canopy. The soil model has six layers, which sum up to 4 m. The land surface module solves the exchange of water vapor, energy, carbon dioxide, and momentum between the ground and vegetation, between different vegetation canopy layers, and between the vegetation canopy and the atmosphere at each canopy level. Also represented in this module are the exchanges of water and energy between different soil layers. The main equations in the land surface module predict the temperature of different vegetation components, the air temperature and specific humidity at each canopy level, and the temperature and soil moisture of each soil layer. To help understand our model results, in the following we describe how the surface hydrology is treated in the model.

The land surface module includes a detailed description for the precipitation cascade. Rain falls over the upper vegetation canopy and part of it gets intercepted, which contributes to the upper canopy storage. The throughfall from the upper canopy, including the instantaneous throughfall and the slow canopy dripping, falls over the lower canopy. Following canopy interception at the lower layer, what reaches the ground is the throughfall from the lower canopy. The intercepted rainfall stays as free water on the wet canopy surface. Dripping and reevaporation reduce the water storage at both canopy layers.

The amount of water that reaches the ground is divided into three parts: direct evaporation from surface puddles, surface runoff that discharges out of the system, and infiltration that recharges the water storage in the soil. Within the soil, water movement between different layers is governed by gravity drainage and diffusion, with three moisture sinks: direct evaporation, plant uptake, and drainage out of the bottom. Direct evaporation from the soil only occurs in the top soil layer. Water uptake by plants from different soil layers depends on the rooting profiles, which are based on published data (Jackson et al. 1996). The drainage from the bottom soil layer is modeled assuming gravity drainage and neglecting interactions with groundwater aquifers.

Within the vegetation canopy, the major component of water vapor exchange is the plant transpiration, which is strongly related to photosynthesis and stomatal conductance. Plant stomata opens during photosynthesis to let CO_2 in. As a result, the stomata loses water to the ambient environment in the form of transpiration. When part of the canopy becomes wet, the photosynthesis is suppressed, which would correspondingly reduce the stomatal conductance and therefore the transpiration. The water for transpiration is supplied through the plant uptake from the soil. Upon water stress, stomatal con-

ductance decreases, therefore the transpiration rate also decreases. When water stress becomes severe enough, drought-deciduous plants shed their leaves to preserve water.

Although the land surface module in IBIS has detailed description of surface hydrology, it does not consider the impact of rainfall subgrid variability. For example, the canopy interception (I) is estimated as a function of the vegetation density [represented by the single-sided leaf area index (LAI)] and does not depend on the subgrid distribution of the rainfall:

$$I = P_0[1 - \exp(-\mathrm{LAI})],$$

where P_0 is the precipitation rate predicted by the atmospheric model, which represents the rainfall average over each grid cell. For greater physical realism, we modified the representation of canopy hydrology by incorporating into it an interception scheme that accounts for the spatial variability in rainfall interception.

c. Interception scheme

We take a statistical approach in representing the subgrid variability of rainfall. Following Shuttleworth (1988), precipitation is assumed to fall over a fraction μ of the grid cell, and the probability distribution of precipitation P within the rain-covered region follows a decaying exponential function, as shown in the following:

$$f(P) = \frac{\mu}{P_0} \exp\left(-\frac{\mu P}{P_0}\right), \tag{2}$$

where P_0 is the grid-averaged precipitation rate. As a result, the grid-averaged rate of canopy interception, which is the part of the grid rainfall that adds to the canopy storage, can be derived (Shuttleworth 1988) as

$$I = P_0\left[1 - \exp\left(-\frac{\mu I_{\max}}{P_0}\right)\right], \tag{3}$$

where $I_{\max} = (S - C)/\Delta t$, with S being the canopy capacity, C the canopy storage, and Δt the model time step. We then compute the grid-average throughfall by summing up the instantaneous throughfall (i.e., $P_0 - I$) and the slow dripping from the canopy storage. This treatment is applied to each layer of the vegetation canopy, with P_0 for the lower layer replaced by the throughfall from the upper-layer canopy.

The choice of the parameter μ may significantly affect the model's climatology. In fact, previous studies (Pitman et al. 1990; Johnson et al. 1991; Thomas and Henderson-Sellers 1991) already showed that a model's climate is indeed sensitive to the choice of μ. Here we use the Eltahir and Bras (1993b) method to estimate the fractional rainfall coverage:

$$\mu = \frac{P_0}{P_{\mathrm{obs}}}, \tag{4}$$

where P_0 is the modeled rainfall intensity, and P_{obs} is the climatology of observed rainfall intensity at the corresponding location and during the corresponding season. We estimate P_{obs} based on published data in Lebel et al. (1997) and Le Barbe and Lebel (1997). This way of estimating μ guarantees that the precipitation intensity in the model is always close to observations, and allows μ to change with time and location, therefore bringing greater physical realism into the model (Eltahir and Bras 1993b).

Compared with treating rainfall as uniformly distributed, the above way of estimating the rainfall interception is based on a more realistic precipitation distribution. However, the heterogeneity of surface properties (e.g., vegetation type and soil texture) is not considered. In addition, although precipitation is spatially variable within a grid, the subgrid variability of canopy storage is not considered, which introduces a certain degree of inconsistency (Eltahir and Bras 1994). Another approximation has to do with the presence of two vegetation layers. The ''rain'' falling over the lower-layer canopy is actually the throughfall from the upper layer. The ''routing'' effect of the upper-layer canopy may significantly modify the rain distribution for the lower canopy. However, in the model, we assume that both the parameter μ and the form of probability distribution function for the lower-layer canopy are the same as the upper-layer canopy. This assumption may cause inaccuracy in regions with savannah-type vegetation (i.e., a mixture of trees and grasses), but imposes no influence over regions with tree-only or grass-only vegetation.

d. Vegetation dynamics module

The vegetation cover in IBIS (Foley et al. 1996) is a combination of different plant functional types (PFTs). PFTs are defined based on physiognomy (tree or grass), leaf form (broad-leaf or needle-leaf), leaf habit (evergreen or deciduous), and photosynthetic pathway (C_3 or C_4). For example, PFTs that grow well in the Tropics include tropical broad-leaf evergreen trees, tropical broad-leaf drought-deciduous trees, and C_4 grasses. Woody plants form the upper layer of the vegetation canopy, and herbaceous plants form the lower layer of the vegetation canopy.

The vegetation dynamics module updates the vegetation structure for each PFT at an annual time step according to the net primary productivity (NPP) of that PFT. The annual NPP is the difference between photosynthesis and respiration, integrated through an entire year. Whether a PFT can potentially exist at a specific location depends on the climatic constraints; whether it can actually survive depends on its competition with other PFTs for common resources. The transient change in vegetation structure, including the LAI and living biomass, is a reflection of this competition. Common resources account for water and light. The effect of nutrient stress is not considered.

PFTs in different vegetation layers have different advantages in accessing light and water. The upper layer has easier access to sunlight, and shades the lower layer to a certain degree depending on its fractional coverage. Plants in the upper layer have deeper root structures than those in the lower layer. As a result, the lower-layer PFTs have the advantage of reaching water first in the process of infiltration, while the upper-layer PFTs have access to the water storage in the deeper soil. In terms of life form, herbaceous plants in the lower layer need not divert resources into the production and maintenance of the woody supporting structures as woody plants in the upper layer do.

Competition between PFTs within the same canopy layer has to do with the differences in their ecological strategies. For example, under severe water stress, drought-deciduous plants shed their leaves to shut off the water consumption through transpiration. Needle leaf plants conserve water better than broad-leaf plants, and C_4 grass uses water more efficiently than C_3 grass. These factors cause differences in carbon balance between different PFTs in the same canopy layer.

3. Experiments design

Taking West Africa as an example, we use ZonalBAM to evaluate the impact of the subgrid variability in rainfall interception. Two experiments, one labeled as variable and one uniform, are performed. In the variable case, the interception scheme presented in section 2c is used; in the uniform case, the interception calculation of original IBIS described in section 2b is used, which assumes uniform rainfall distribution over each grid cell.

The land–ocean boundary in ZonalBAM is set at 6°N, with land in the north and ocean in the south. Over the ocean, sea surface temperature is fixed at its climatological value averaged over 15°W–15°E. Over the land, static vegetation is used at this stage—the role of vegetation dynamics will be addressed later in this study. Here the static vegetation implies only that the vegetation structure does not change from one year to the next. Diurnal cycle and seasonal cycle still exist in the plant physiological and phenological processes.

In the experiments here, forest occupies the region between the coast and 12.5°N, with rain forest near the coast and drought-deciduous forest northward; grassland extends from 12.5°N to the desert border near 17.5°N, with dense tall grass near the forest and short grass near the desert. The northern boundary of the desert is set at 27°N. Beyond the Tropics (27°S–27°N), the land surface temperature and fluxes are fixed at their climatology based on the National Centers for Environmental Prediction (NCEP) reanalysis data (1958–97; Kalnay et al. 1996). The above-specified vegetation distribution over West Africa is similar to, but slightly different from, the observations (Foley et al. 1996; Gornitz and NASA 1985). Reaching as far north as 12.5°N, the drought-deciduous forest in the model covers both the dry forest region and the savannah region of today's West Africa. Vegetation specified in the model is either forest or grassland, without any mixture of trees and grass. Therefore, the assumption that the subgrid ''rainfall'' variability for the lower canopy is the same as the upper canopy does not affect our experiments. Moreover, the increase of forest-covered region makes the effect of rainfall subgrid variability more distinguishable since trees have a higher canopy capacity than other vegetation forms.

In both the uniform and variable experiments, a time step of 20 min is used. The horizontal resolution is close to 2.5° in the Tropics and the vertical resolution is about 40 mb. Three years of integration is needed before the model reaches equilibrium. Additional simulation reveals neither noticeable trend nor noticeable interannual variability. Therefore, in the following we present the results from the fourth year of the simulation. Since the model with the interception scheme presented in section 2c has been successfully tested against observations (Wang and Eltahir 2000a), our interest in this study is not in how well each of the experiments reproduces the observed climate. Instead, here we focus on the simulation differences that result from the assumption of uniform rainfall distribution. For the purpose of this study, we concentrate only on the region of West Africa between 6°N (the coast) and 20°N (desert).

4. Analysis of results

a. Main results

Here we present our results through comparison between the two experiments: the variable experiment, which considers the rainfall subgrid variability, and the uniform experiment, which assumes uniform distribution of rainfall within each grid cell.

Results on surface hydrology are presented in Figs. 1a–d. Figures 1a and 1b show the interception loss and transpiration, respectively. The uniform case overestimates the interception loss by more than 100%, and significantly underestimates the plant transpiration over the forest region. The difference over the grassland region is not as significant. Figures 1c and 1d present the evapotranspiration and runoff, respectively. Despite the dramatic difference in the partitioning between interception loss and transpiration, the overall evapotranspiration remains the same over the forest region. Over the grassland region in the uniform case, an increase of evapotranspiration is observed. Although the total evapotranspiration is rather insensitive to rainfall interception, a significant difference is observed in runoff. Runoff, which is up to 725 mm yr^{-1} in the variable case, is almost nonexistent in the uniform case. Our results over the forest region, including the overestimation of interception loss, underestimation of transpiration, and more importantly, the low sensitivity of the total evapotranspiration, are consistent with the findings of Dolman

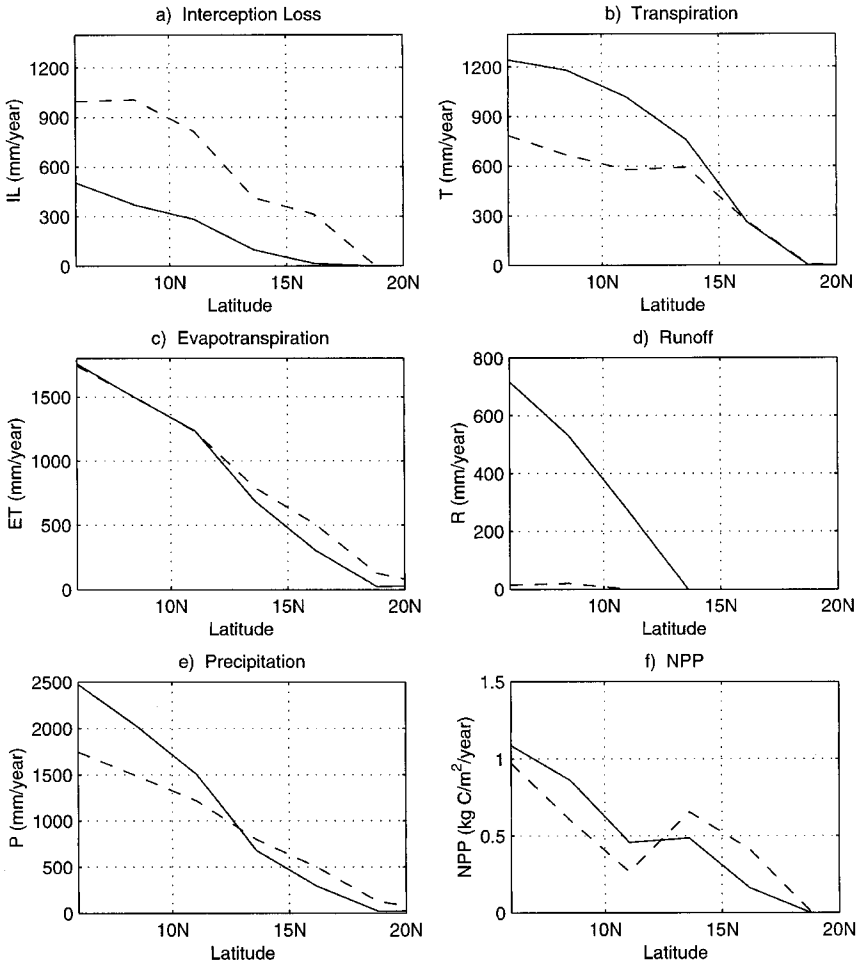

FIG. 1. The comparison between the uniform case (dashed line) and the variable case (solid line) for (a) interception loss, (b) transpiration, (c) evapotranspiration, (d) total runoff, (e) precipitation, and (f) net primary productivity. The annual accumulation is presented for all variables.

and Gregory (1992). It is important to note that the Dolman and Gregory (1992) study also used a coupled land surface–atmosphere model. This agreement suggests that the high sensitivity of total evapotranspiration to rainfall interception found in studies using offline land surface models may have to do with the lack of atmospheric feedback.

The bias caused by neglecting the rainfall subgrid variability is not limited to the surface hydrological processes. It also affects the simulation of biospheric and atmospheric processes to a great degree, as shown by Figs. 1e,f. Figure 1e presents precipitation as an example for the atmospheric climate, and Fig. 1f presents the NPP as an example for the biospheric climate. Although the total evapotranspiration remains the same, comparison of the precipitation between the two experiments shows a striking difference. Precipitation is underestimated in the uniform case by up to 35% in the forest region, and significantly overestimated in the grassland region. Correspondingly, in the biosphere, NPP is underestimated in the forest region and overestimated in the grassland region.

In the following we focus on interpreting the results presented above, in particular, on understanding how errors in the representation of rainfall interception propagate into the atmosphere and the biosphere although the total evapotranspiration is correctly simulated. As shown by Figs. 1e,f, the response of the biosphere–atmosphere system differs between the forest region and the grassland region. Therefore these two regions are analyzed separately in the following.

b. Interpretation of results for the forest region

To understand the impact of rainfall subgrid variability, we start from the micrometeorological processes within the vegetation canopy. When falling uniformly over the entire model grid cell whose size is orders larger than the size of a typical rain cell, rainfall occurs

in the form of drizzle. The small raindrops tend to stay on the leaves. Therefore, the amount of free water on the canopy, as well as the wet canopy area, increases. Similar to the the change from the land to the ocean, the easily accessible water on the canopy favors a moister and cooler environment within the canopy. Consequently, humidity of the air within the canopy increases, and canopy temperatures, including the leaf temperature and stem temperature, decrease. As an example, Fig. 2a shows the fraction of wet leaf area on a typical day of August, which is larger in the uniform case due to the extra wetting effect; the corresponding leaf temperature and canopy air humidity on that same day are presented in Figs. 2b,c. Clearly, for the uniform case, the canopy is cooler and the air within the canopy is moister.

The rate of evaporation (E) from the intercepted water over a unit wet leaf area is proportional to the moisture deficit $Q_s - Q_a$, where Q_s is the saturation specific humidity at the canopy temperature, and Q_a is the specific humidity of the canopy air. For the uniform case, both the lower temperature of the canopy and the moister air within the canopy favor a smaller moisture deficit. As a result, E over a unit wet leaf area is lower in the uniform case. However, the wet leaf area is larger in the uniform case. As shown in Fig. 2a, the wetting fraction at 6°N is about 2.5% for the variable case, but is more than 10% for the uniform case. This significant increase of wetness (by a factor of more than 3) dominates over the impact of reduced moisture deficit, thus causing a higher interception loss in the uniform case (Fig. 1a).

The rate of plant transpiration (T) is proportional to the stomatal conductance K_s and the humidity deficit $Q_{sl} - Q_a$, where Q_{sl} is the saturation specific humidity at the leaf temperature, and Q_a is the specific humidity of the canopy air. Similar to the effect on E, the canopy environment in the uniform case favors a smaller moisture deficit. At the same time, due to the excessive wetness in the uniform case, less leaf area is available for the absorption of photons. As a result, the photosynthesis rate decreases, which causes a decrease in plant stomatal conductance K_s. The reductions in both $Q_{sl} - Q_a$ and K_s contribute to the lower transpiration in the uniform case, as observed in Fig. 1b.

The total evapotranspiration has three components: interception loss, transpiration, and soil evaporation. Over the forest region, soil evaporation is negligible. Interception loss and transpiration count for most of the evapotranspiration. The increase of interception loss and the decrease of transpiration compensate for each other, thus bringing the total evapotranspiration for the uniform case close to the variable case (Fig. 1c). This mechanism is described by the flowchart in Fig. 3. Here we would like to emphasize that it is physically possible for a climate model to have severe errors in the description of surface hydrology but still get accurate simulation of the total evapotranspiration. What makes this issue critical is the fact that these errors are not limited to the land surface. Instead, they propagate into the atmosphere and the biosphere through feedback mechanisms as analyzed in the following.

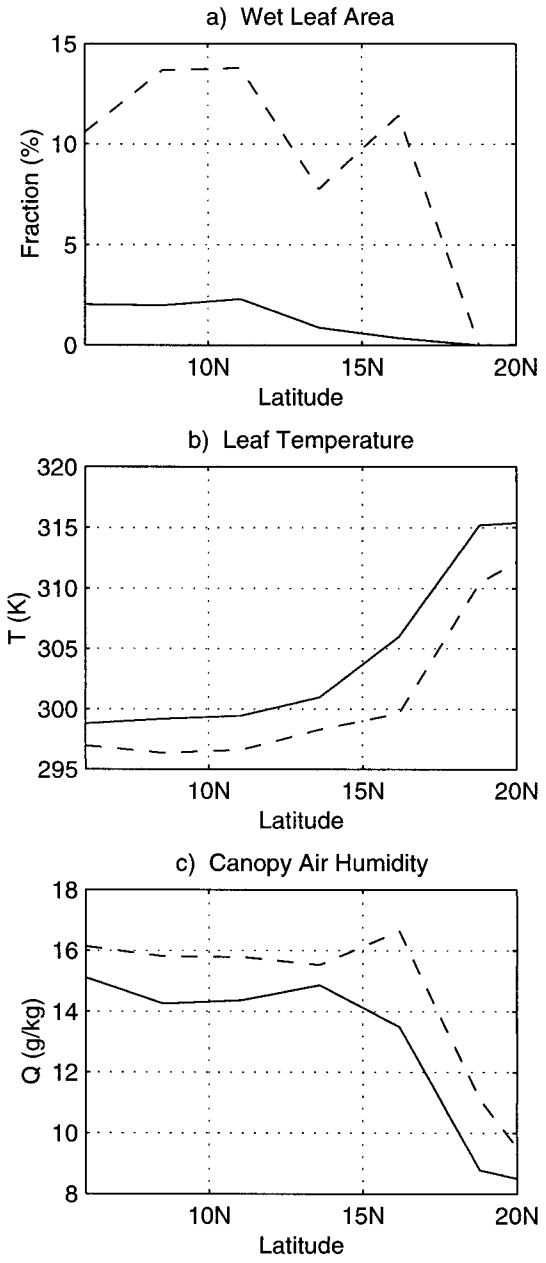

FIG. 2. The comparison between the uniform case (dashed line) and the variable case (solid line) for the canopy condition in Aug (rainy season): (a) fraction of the leaf area that is wet, (b) leaf temperature, and (c) specific humidity of the canopy air.

For the atmosphere in the uniform case, the higher humidity of the canopy air favors a higher rate of water vapor flux into the overlying atmosphere, thus having a moistening effect; the lower vegetation temperature tends to reduce the sensible heat flux, thus causing a cooling effect. As the low-level atmosphere gets moister

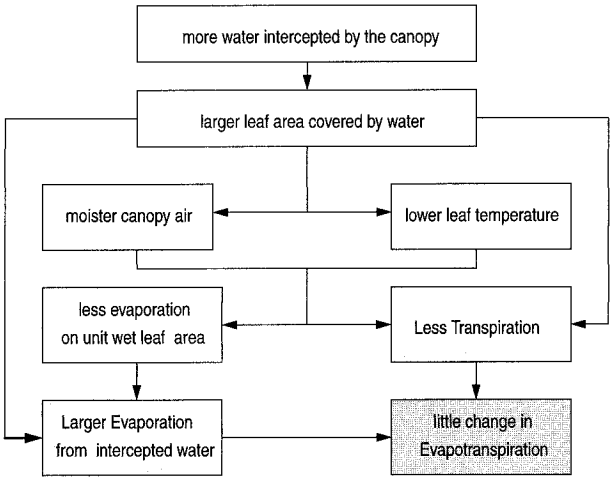

FIG. 3. A mechanism through which the representation of subgrid variability influences the simulation of surface hydrology. The connection between the ''larger leaf area covered by water'' and ''less transpiration'' is through the photosynthesis and stomatal conductance.

and cooler, more low-level clouds will form. Figure 4 presents the fractional cover of low-level clouds during August. The increase of low-level clouds reduces not only the incoming solar radiation at the land surface but also the surface net radiation (Slingo 1990; Klein and Hartmann 1993; Baker 1997), as shown in Figs. 5a,b. This cloud feedback further enhances the sensible heat flux reduction initiated by the reduced canopy temperature. It also tends to suppress the evapotranspiration, which may offset the increase initiated by the overestimated canopy wetness. As a result, the sensible heat flux in the uniform case is lower, but very little difference in the latent heat flux is observed (Fig. 5c). Therefore, the total energy flux from the land surface to the atmosphere is lower in the uniform case by up to 15 W m^{-2}.

In the uniform case, there is less energy flux from the land surface to the atmospheric boundary layer,

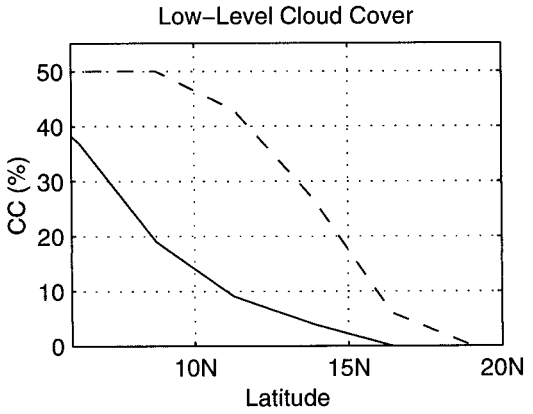

FIG. 4. The fractional cover of low-level clouds in the uniform case (dashed line) and the variable case (solid line).

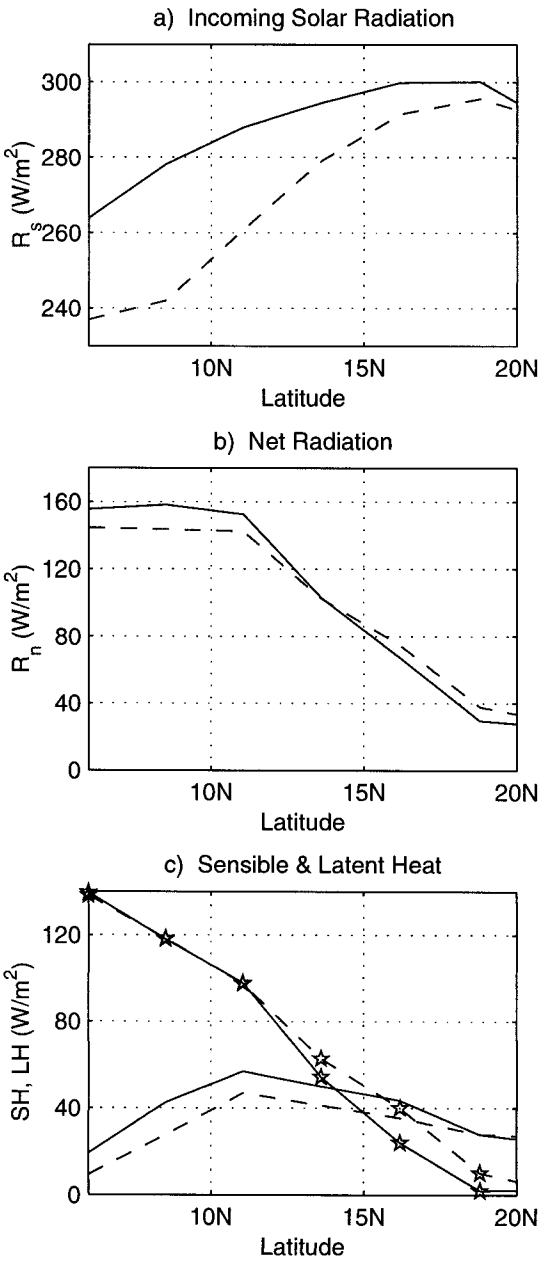

FIG. 5. The comparison between the uniform case (dashed line) and the variable case (solid line) for energy fluxes at the surface: (a) incoming solar radiation, (b) net radiation, and (c) sensible heat flux (plain line) and latent heat flux (line with pentagram). The annual average is presented for the variables.

which tends to stabilize the atmosphere. As a result, the intensity of atmospheric convection decreases, and so does the precipitation falling to the surface (Fig. 1e). Since the evapotranspiration remains the same, the reduction of precipitation signals a decrease of moisture convergence due to changes in the large-scale circulation, which is, in this case, the West African monsoon circulation. As demonstrated before, the assumption of uniform rainfall distribution causes underestimation of

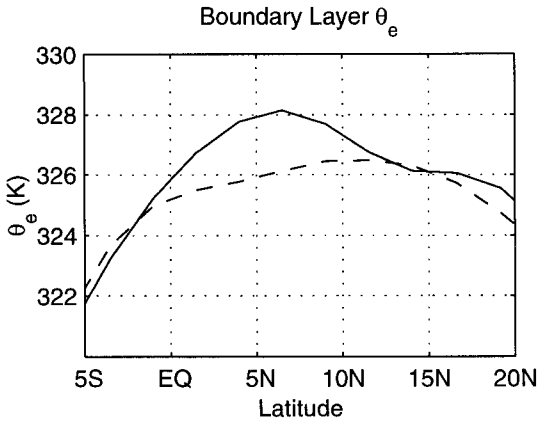

FIG. 6. The equivalent potential temperature θ_e for the uniform case (dashed line) and the variable case (solid line) averaged between 1000 and 800 mb. Here θ_e can be viewed as an index of the boundary layer entropy Θ: $\Theta = C_p \ln\theta_e +$ constant.

total surface energy flux, which is the energy supply for the atmospheric boundary layer. This would tend to reduce the moist static energy supplied to the atmospheric boundary layer. At the same time, the depth of the boundary layer over forest would be smaller in the uniform case due to the reduction in sensible heat flux (Fig. 5). This effect would tend to increase the magnitude of the moist static energy per unit depth. It seems that the effect of the decrease in the total flux of heat is larger than the effect of the change in boundary layer depth. Therefore, the boundary layer moist static energy and entropy over the forest region are underestimated (Eltahir 1996). As a result, in the uniform case, the boundary layer entropy gradient from the ocean toward the land is smaller, and the peak of the boundary layer entropy moves northward (Fig. 6). During the monsoon season, such differences favor a monsoon circulation that is weaker (Eltahir and Gong 1996) but penetrates farther inland. This can be clearly demonstrated by Figs. 7a–d. According to Figs. 7a,b, the low-level meridional wind across the coast is weaker in the uniform case than in the variable case; at the same time, as shown in Figs. 7c,d, the rising motion over the land is weaker in the uniform case, and its peak occurs further northward. These changes in the monsoon circulation cause a decrease of rainfall over the forest region in the south. In the land surface water budget, the precipitation reduction is balanced by the runoff decrease (Fig. 1d).

The difference in NPP between the uniform case and the variable case (Fig. 1f) is closely related to two factors: leaf wetting and clouds. As mentioned above, in the uniform case, the excessive canopy wetness leaves less area available for photosynthesis. At the same time, the increase of low-level clouds reduces the incoming solar radiation, therefore reduces the photosynthetically

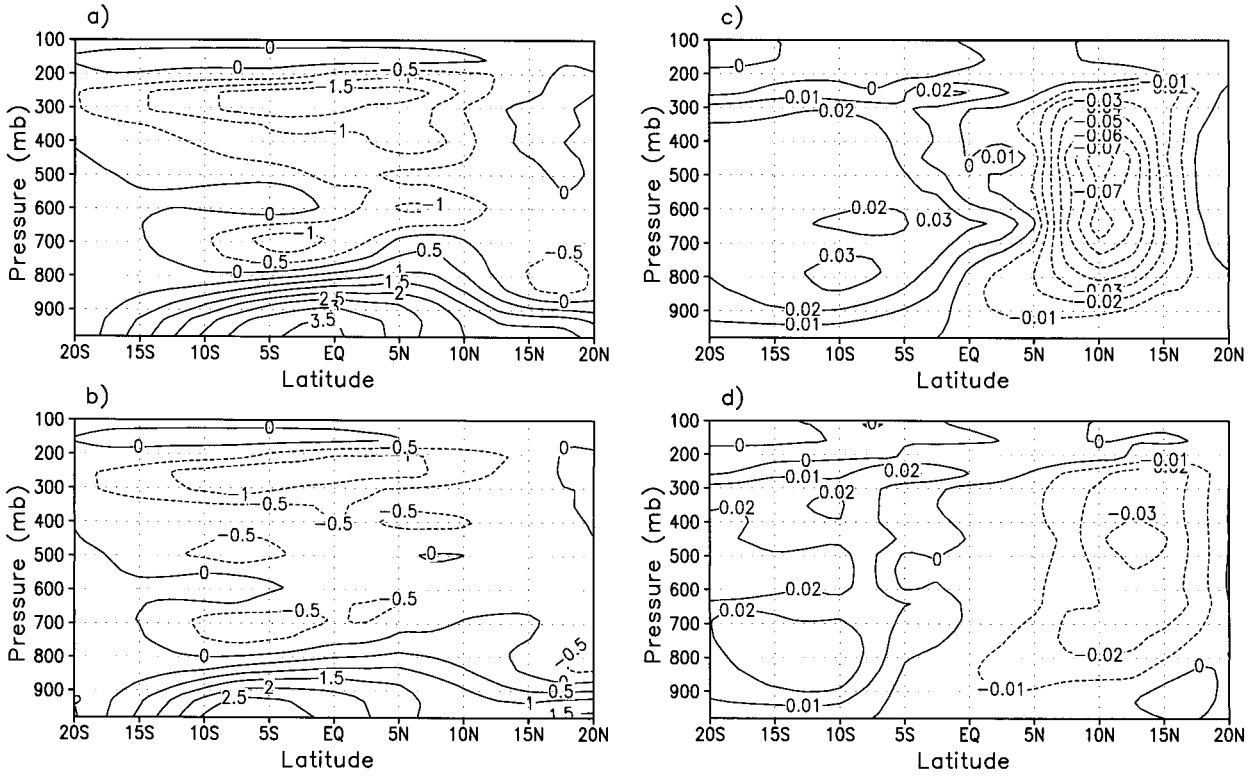

FIG. 7. The meridional circulation in Aug (rainy season): (a) meridional wind (m s^{-1}) field for the variable case, (b) meridional wind (m s^{-1}) field for the uniform case, (c) vertical velocity (Pa s^{-1}) for the variable case, and (d) vertical velocity (Pa s^{-1}) for the uniform case.

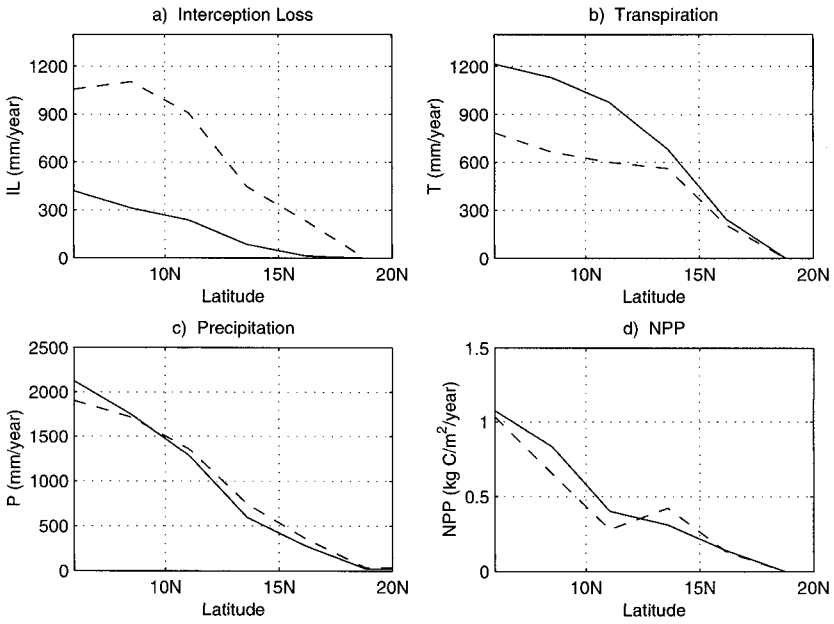

FIG. 8. The comparison between the uniform case (dashed line) and the variable case (solid line) for (a) interception loss, (b) transpiration, (c) precipitation, and (d) net primary productivity. Similar to Fig. 1 but with prescribed cloud cover, and the cloud fractional cover in the uniform case is the same as in the variable case. The annual accumulation is presented for all variables.

active radiation. Both of these two factors cause lower photosynthesis rate, thus lower NPP.

In addition to the above-mentioned effects, another important mechanism has to do with the water availability in the root zone. Over the forest region in the uniform case, both the overestimation of interception loss and the underestimation of precipitation reduces the water availability in the root zone. The resulting water stress will further suppress the plant photosynthesis and transpiration. However, this effect may not be significant since the plant growth over forest region is more frequently limited by light availability instead of water availability.

c. Interpretation of results for the grassland region

The physical mechanisms responsible for the error propagation over the forest region are also valid over the grassland region. However, these local factors may not play the dominant role in the grassland region, according to Figs. 1e,f. Climate over West Africa is under the influence of the West African monsoon circulation. As demonstrated in Fig. 7, the assumption of uniform rainfall distribution causes a monsoon circulation that is weaker but penetrates further inland, which results in a northward expansion of the monsoon rain belt at the expense of a rainfall decrease in the south. Therefore, over the grassland in the north, rainfall is overestimated in the uniform case (Fig. 1e). As a response to this excessive water availability, the total evapotranspiration and NPP are all overestimated (Fig. 1).

5. Role of cloud feedback in error propagation

Analyses in section 4 suggest that cloud feedback plays an important role in propagating the errors associated with the misrepresentation of rainfall interception. To further validate our interpretation, here we investigate the sensitivity of the model results to the cloud feedback by conducting two experiments, one uniform, and one variable. These two experiments are the same as their counterparts described in section 3 but without the cloud feedback, that is, the cloud cover for the experiments of this section is prescribed, instead of being predicted by the model. Here the fractional cloud covers in both experiments are fixed at the same value, which is derived from the seasonal cycle of the cloud covers predicted by the variable experiment in section 3.

The role of cloud feedback in error propagation can be demonstrated from comparisons between experiments with prescribed clouds (in this section) and those with interactive clouds (in section 3). Figures 8a,b present the results for the interception loss and transpiration at the same scale as Figs. 1a,b; Figs. 8c,d present the results for the precipitation and NPP at the same scale as Figs. 1e,f. Although a significant difference between the uniform case and the variable case still exists in the partition of evapotranspiration, the differences in precipitation as well as in NPP are much smaller when no cloud feedback is allowed (Figs. 8c,d, compared with Figs. 1e,f). The cloud feedback is responsible for most of the precipitation difference between the uniform case and the variable case shown in Fig. 1e. Of the difference

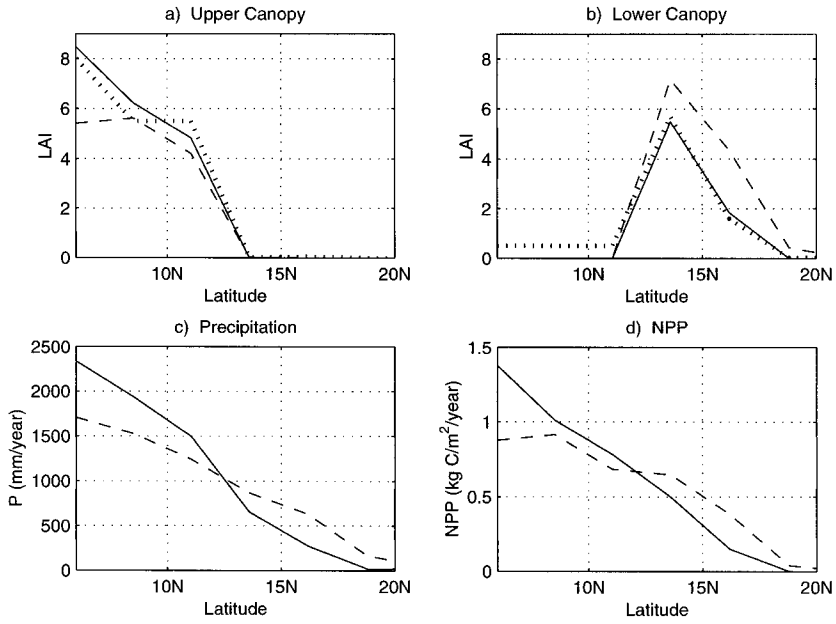

FIG. 9. Comparison of the equilibrium state between the uniform case (dashed line) and the variable case (solid line). (a) The growing-season LAI for the upper canopy, (b) the growing-season LAI for the lower canopy, (c) annual precipitation, and (d) annual net primary productivity. The dotted line in (a) and (b) represents the growing-season LAI at the initial condition.

in NPP (Fig. 1f), about one-half is attributed to the cloud feedback.

6. Error propagation through vegetation dynamics

In the above simulations, we used a static vegetation distribution and did not consider the effect of vegetation dynamics. However, since the representation of rainfall subgrid variability affects the estimation of the NPP, further error propagation is expected when vegetation dynamics are included. To address this issue, we perform two experiments, one uniform and one variable, which are the same as the experiments described in section 3 but with dynamic vegetation. The vegetation distribution described in section 3 is used as the initial vegetation condition. The biosphere–atmosphere system is then allowed to evolve toward its equilibrium state through the two-way feedback between the biosphere and the atmosphere.

It takes three to four decades for each of the simulations in both experiments to reach an equilibrium. Here we use the LAI, precipitation, and NPP to represent the equilibrium state. Figure 9a presents the growing-season LAI for trees at the equilibrium in both the uniform and the variable experiments, compared with the initial condition. Figure 9b is the same as Fig. 9a but for herbaceous plants. In general, trees in the variable experiment grow denser but become less dense in the uniform experiment. In contrast, the herbaceous plants in the uniform case are significantly denser than the initial condition. These results are consistent with the comparison of NPP in Fig. 1f, which shows that NPP is underestimated over the forest region and overestimated over the grassland region when the rainfall subgrid variability is neglected. The vegetation changes in both experiments are associated with other changes in the biosphere–atmosphere system. For example, Figs. 9c,d show the precipitation and NPP at equilibrium in both the uniform and the variable experiments. Comparing Figs. 9c,d with Figs. 1e,f suggests that the differences in both the precipitation and NPP between the uniform case and the variable case are enhanced by vegetation dynamics, especially over the grassland region. The bias caused by neglecting the rainfall subgrid variability drives the biosphere–atmosphere system into a significantly different equilibrium state. This is highlighted by the differences in annual rainfall and NPP (up to a factor of 2) documented in Figs. 9c,d.

7. Discussion and conclusions

In this paper, using West Africa as a case study, we investigate the impact of the subgrid variability in rainfall interception using a coupled biosphere–atmosphere model. This study provides evidence for the need to have physical realism in modeling the coupled biosphere–atmosphere–ocean system. One finding of this study is that a climate model may succeed in accurately simulating the total evapotranspiration while misrepresenting the canopy hydrology. In addition, this bias in the canopy hydrology would introduce significant errors in the broad aspects of the biosphere–atmosphere

system. Several conclusions can be drawn from our results.

1) Neglecting the subgrid variability in rainfall interception may not cause noticeable bias in the simulation of total evapotranspiration. However, interception loss is significantly overestimated and transpiration is significantly underestimated. At the same time, runoff is significantly underestimated.
2) Even though the total evapotranspiration remains the same, the error in its partitioning between direct evaporation and transpiration (as stated above in item 1) causes significant differences in the atmospheric processes: moister atmosphere, more low-level clouds, smaller total (sensible plus latent) heat flux, and weaker monsoon circulation. These errors result in an underestimation of precipitation over the forest region in West Africa. However, over the grassland region, an overestimation of precipitation results from the dominance of large-scale factors involving the monsoon circulation over local factors.
3) Among biospheric processes, NPP over the forest region is significantly underestimated when the subgrid variability in rainfall interception is neglected. Over the grassland region where plant growth is limited by water availability, NPP is overestimated due to the overestimation of precipitation.
4) The low-level cloud feedback plays an important role in propagating the errors in the representation of rainfall interception to both the atmospheric processes and the biospheric processes.
5) Vegetation dynamics further propagate the resultant errors by changing the state of the biosphere, which then feeds back to the atmosphere and eventually leads to a different biosphere–atmosphere equilibrium. This equilibrium features denser vegetation in the grassland region but less dense vegetation in the forest region.

While previous studies focused on the impact of subgrid variability on the simulation of land surface processes, the investigation of our study extends to the broad aspects of climate modeling including the simulation of the biosphere, the atmosphere, and the biosphere–atmosphere equilibrium. In addition, we have devoted a considerable effort to understanding the mechanisms of the error propagation. However, at this stage we focused only on the subgrid variability in rainfall interception and did not consider the heterogeneity of land surface properties. Also, there has been no consideration for the impact of rainfall subgrid variability on the infiltration and runoff generation. The lack of treatment for these subgrid land surface processes and properties may have an impact on the general applicability of the results from this study. The representation of land surface heterogeneity has been investigated by several studies (Koster and Suarez 1992a,b; Seth et al. 1994; Giorgi and Avissar 1997; Giorgi 1997), but most of these studies used offline land surface models and focused on the impact of subgrid heterogeneity on land surface processes. In future research, we plan to study the broad impact of land surface heterogeneity using a coupled biosphere–atmosphere model.

Acknowledgments. We thank Dr. Jonathan Foley and his group at the University of Wisconsin for sharing the biospheric model IBIS. We are grateful to Julie Kiang for suggestions and discussions. We also thank the two anonymous reviewers for their helpful comments. NCEP reanalysis data were provided by the NOAA–CIRES Climate Diagnostics Center, Boulder, Colorado. This research has been supported by the National Aeronautics and Space Administration (NASA) under Agreement NAGW-5201, NAG5-7525, and NAG5-8617, and by the National Science Foundation (NSF) under Agreement ATM 9807068. The views, opinions, and/or findings contained in this paper are those of the authors and should not be construed as an official NASA or NSF position, policy, or decision, unless so designated by other documentation.

REFERENCES

Avissar, R., and R. A. Pielke, 1989: A parameterization of heterogeneous land surfaces for atmospheric numerical models and its impact on regional meteorology. *Mon. Wea. Rev.*, **117,** 2113–2136.

Baker, M. B., 1997: Cloud microphysics and climate. *Science,* **276,** 1072–1078.

Carson, D. J., 1986: Parameterization of land surface processes in meteorological office numerical weather predicting and climate models. Dynamical Climatology Tech. Note 37, 30 pp. [Available from U.K. Met. Office, London Rd., Bracknell, Berkshire, RG12 2SZ, United Kingdom.]

Dickinson, R. E., A. Henderson-Sellers, and P. J. Kennedy, 1993: Biosphere–Atmsophere Transfer Scheme (BATS) Version 1e as coupled to the NCAR Community Climate Model. NCAR Tech. Note NCAR/TN-387+STR, 72 pp.

Dolman, A. J., and D. Gregory, 1992: The parameterization of rainfall interception in GCMs. *Quart. J. Roy. Meteor. Soc.*, **118,** 455–467.

Eltahir, E. A. B., 1996: Role of vegetation in sustaining large-scale atmospheric circulations in the Tropics. *J. Geophys. Res.*, **101** (D2), 4255–4268.

——, and R. L. Bras, 1993a: Estimation of the fractional coverage of rainfall in climate models. *J. Climate,* **6,** 639–644.

——, and ——, 1993b: Description of rainfall interception over large areas. *J. Climate,* **6,** 1002–1008.

——, and ——, 1994: Comments on ''The parameterization of rainfall interception in GCMs.'' *Quart. J. Roy. Meteor. Soc.,* **120,** 733–734.

——, and C. Gong, 1996: Dynamics of wet and dry years in West Africa. *J. Climate,* **9,** 1030–1042.

Entekhabi, D., and P. S. Eagleson, 1989: Land surface hydrology parameterization for atmospheric general circulation models including subgrid scale spatial variability. *J. Climate,* **2,** 816–831.

Foley, J. A., I. C. Prentice, N. Ramankutty, S. Levis, D. Pollard, S. Sitch, and A. Haxeltine, 1996: An integrated biosphere model of land surface processes, terrestrial carbon balance, and vegetation dynamics. *Global Biogeochem. Cycles,* **10,** 603–628.

Ghan, S. J., J. C. Liljegren, W. J. Shaw, J. H. Hubbe, and J. C. Dorman, 1997: Influence of subgrid variability on surface hydrology. *J. Climate,* **10,** 3157–3166.

Giorgi, F., 1997: An approach for the representation of surface het-

erogeneity in land surface models. Part 2: Validation and sensitivity experiments. *Mon. Wea. Rev.,* **125,** 1900–1919.
——, and R. Avissar, 1997: Representaion of heterogeneity effects in earth system modeling: Experience from land surface modeling. *Rev. Geophys.,* **35,** 413–438.
Gornitz, V., and NASA, 1985: A survey of anthropogenic vegetation changes in West Africa during the last century—Climatic implications. *Climatic Change,* **7,** 285–325.
Jackson, R. B., J. Canadell, J. R. Ehleringer, H. A. Mooney, O. E. Sala, and E. D. Schulze, 1996: A global analysis of root distributions for terrestrial biomes. *Oecologia,* **108,** 389–411.
Johnson, K. D., D. Entekhabi, and P. S. Eagleson, 1991: The implementation and validation of improved landsurface hydrology in an atmospheric general circulation model. Ralph M. Parsons Laboratory Tech. Rep. 334, 192 pp. [Available from Ralph M. Parsons Laboratory, Massachusetts Institute of Technology, Cambridge, MA 02139.]
Kalnay, E., and Coauthors, 1996: The NCEP/NCAR 40-year reanalysis project. *Bull. Amer. Meteor. Soc.,* **77,** 437–471.
Kim, C. P., and D. Entekhabi, 1998: Feedbacks in the land-surface and mixed-layer energy budgets. *Bound.-Layer Meteor.,* **88,** 1–21.
Klein, S. A., and D. L. Hartmann, 1993: The seasonal cycle of low stratiform clouds. *J. Climate,* **6,** 1587–1606.
Koster, R. D., and M. J. Suarez, 1992a: Modeling the land-surface boundary in climate models as a composite of independent vegetation stands. *J. Geophys. Res.,* **97,** 2697–2715.
——, and ——, 1992b: A comparative analysis of two land surface heterogeneity representations. *J. Climate,* **5,** 1379–1390.
Kvamsto, N. G., 1991: An investigation of diagnostic relations between stratiform fractional cloud cover and other meteorological parameters in numerical weather prediction models. *J. Appl. Meteor.,* **30,** 200–216.
Lean, J., and D. A. Warrilow, 1989: Simulation of the regional climatic impact of Amazon deforestation. *Nature,* **342,** 411–413.
Le Barbe, L., and T. Lebel, 1997: Rainfall climatology of the HAPEX-Sahel region during the years 1950–1990. *J. Hydrol.,* **189,** 43–73.
Lebel, T., J. D. Taupin, and N. D'Amato, 1997: Rainfall monitoring during HAPEX-Sahel. 1. General rainfall conditions and climatology. *J. Hydrol.,* **189,** 74–96.
Lloyd, C. R., 1990: The temporal distribution of Amazonian rainfall and its implications for forest interception. *Quart. J. Roy. Meteor. Soc.,* **116,** 1487–1494.
London, J., 1952: The distribution of radiational temperature change in the Northern Hemisphere during March. *J. Meteor.,* **9,** 145–151.
Mocko, D. M., and W. R. Cotton, 1995: Evaluation of fractional cloudiness parameterizations for use in a mesoscale model. *J. Atmos. Sci.,* **52,** 2884–2901.
Pitman, A. J., A. Henderson-Sellers, and Z.-L. Yang, 1990: Sensitivity of regional climates to localized precipitation in global models. *Nature,* **346,** 734–737.
Pollard, D., and S. L. Thompson, 1995: Use of a land-surface transfer scheme (LSX) in a global climate model: The response to doubling stomatal resistance. *Global Planet. Change,* **10,** 129–161.
Rodriguez-Iturbe, I., and P. S. Eagleson, 1987: Mathematical models of rainstorm events in space and time. *Water Resour. Res.,* **23,** 181–190.
Seth, A., F. Giorgi, and R. E. Dickinson, 1994: Simulating fluxes from heterogeneous land surfaces: Explicit subgrid method employing the biosphere–atmosphere transfer scheme (BATS). *J. Geophys. Res.,* **99,** 18 651–18 667.
Shuttleworth, W. J., 1988: Macrohydrology—The new challenge for process hydrology. *J. Hydrol.,* **100,** 31–56.
Slingo, A., 1990: Sensitivity of the earth's radiation budget to changes in low clouds. *Nature,* **343,** 49–51.
Thomas, G., and A. Henderson-Sellers, 1991: An evaluation of proposed representations of subgrid hydrologic processes in climate models. *J. Climate,* **4,** 898–910.
Wang, G., and E. A. B. Eltahir, 1998: Biosphere–atmosphere interactions: Representation of sub-grid spatial variability of rainfall interception (abstract). *Eos, Trans. Amer. Geophys. Union,* **79,** 349.
——, and ——, 2000a: Biosphere–atmosphere interactions over West Africa. 1. Development and validation of a coupled dynamic model. *Quart J. Roy. Meteor. Soc.,* **126,** 1239–1260.
——, and ——, 2000b: Biosphere–atmosphere interactions over West Africa. 2. Multiple climate equilibria. *Quart. J. Roy. Meteor. Soc.,* **126,** 1261–1280.
Zheng, X., and E. A. B. Eltahir, 1997: The response to deforestation and desertification in a model of West African monsoons. *Geophys. Res. Lett.,* **24,** 155–158.
——, and ——, 1998: The role of vegetation in the dynamics of West African monsoons. *J. Climate,* **11,** 2078–2096.